New Journal of Physics
The open-access journal for physics

Laser spectroscopy by a radiofrequency measurement on a single ion in a Penning trap

M Vogel[1,3] **and W Quint**[2]
[1] Imperial College London, London SW7 2AZ, UK
[2] GSI, Planckstrasse 1, 64291 Darmstadt, Germany
E-mail: m.vogel@gsi.de

New Journal of Physics **11** (2009) 013024 (12pp)
Received 11 September 2008
Published 20 January 2008
Online at http://www.njp.org/
doi:10.1088/1367-2630/11/1/013024

Abstract. We present a novel concept for precision laser spectroscopy on a single ion confined in a Penning trap. This concept circumvents the need for detection of fluorescence photons. Instead, changes in motional frequencies of the trapped ion are used to determine atomic transitions of interest with relative accuracies better than 10^{-10}. We discuss the application to a measurement of forbidden transitions in highly charged ions, making stringent tests of bound-state quantum electrodynamics (QED) calculations, including the nuclear recoil contribution, possible. The method may also be used to 'weigh' optical excitations in light ions by the relativistic frequency shift.

Contents

[3] Author to whom any correspondence should be addressed.

1. Introduction

For laser spectroscopy of atomic or molecular transitions numerous techniques have been conceived and successfully applied, an overview is given for example in [1]. Most often, detection of fluorescence photons upon initial excitation is used to determine the properties of the corresponding transition. Confined single particles have previously been used for highly precise determinations of fundamental quantities [2]–[10] and of atomic transition frequencies [11]–[13].

Laser systems are available within a broad range of frequencies [1] and featuring bandwidths down to the sub-Hz domain [14, 15]. This yields widespread possibilities for excitation of desired transitions. However, especially in the infrared domain, detection of fluorescence photons emitted by trapped particles can be very difficult or even impossible due to a lack of well-suited detectors which can be operated in magnetic fields and/or cryogenic surroundings. As a matter of fact, previous measurements of forbidden transitions in highly charged ions have to a large extent suffered from a bad signal-to-noise ratio in the optical detection, as will be discussed below.

Here, we present a method for laser spectroscopy on a single confined ion which does not rely on detection of fluorescence photons, but rather on a measurement of ion oscillation frequencies in the trap. Thus, no optical detection system is required which in the case of in-trap spectroscopy reduces the experimental effort tremendously. The method combines laser cooling of stored ions [16]–[18] with techniques for ion confinement, manipulation and precision measurements of single-ion properties in Penning traps [16, 19, 20]. Although the present method is, in principle, applicable to any trapped ion suited for laser cooling, we will focus on high-precision measurements of forbidden transitions (i.e. fine structure (FS) and hyperfine structure (HFS) transitions) in highly charged ions. Of specific interest are ground-state hyperfine transitions in hydrogen-like and lithium-like heavy ions such as e.g. $^{209}Bi^{82+}$ and $^{209}Bi^{80+}$ as well as FS transitions in boron-like and carbon-like medium-heavy ions such as e.g. $^{40}Ar^{13+}$ and $^{40}Ar^{12+}$.

2. Spectroscopy of forbidden transitions in highly charged ions

A measurement of the ground-state FS and HFS splitting in a highly charged ion represents a sensitive test of calculations in the framework of quantum electrodynamics of bound states. Calculations of the hyperfine splitting in hydrogen- and lithium-like ions have reached a high accuracy [21]–[27]. By a comparison of the ground state HFS in different charge states of the same isotope all nuclear effects can be ruled out to first order [28]. This allows for bound-state quantum electrodynamics (QED) effects to be isolated and measured with unprecedented accuracy. A precision measurement of FS transitions in highly charged ions allows QED effects including the nuclear recoil contribution to be tested.

The energy of the ground-state hyperfine splitting in highly charged ions scales with the third power of the nuclear charge Z and is accessible by lasers for many ions with $Z > 60$ [25]. There are FS transitions with $n = 2$, $j = 3/2 \rightarrow 1/2$ in the optical domain for various boron- and carbon-like ions with $10 \lesssim Z \lesssim 25$. A limited number of FS transitions in fluor- and beryllium- and oxygen-like ions are in the optical domain as well [29]. To give an overview of possible candidates for investigations, figure 1 shows the estimated wavelengths of FS and HFS transitions in the laser-accessible region for stable and close-to-stable ions (nuclear lifetime

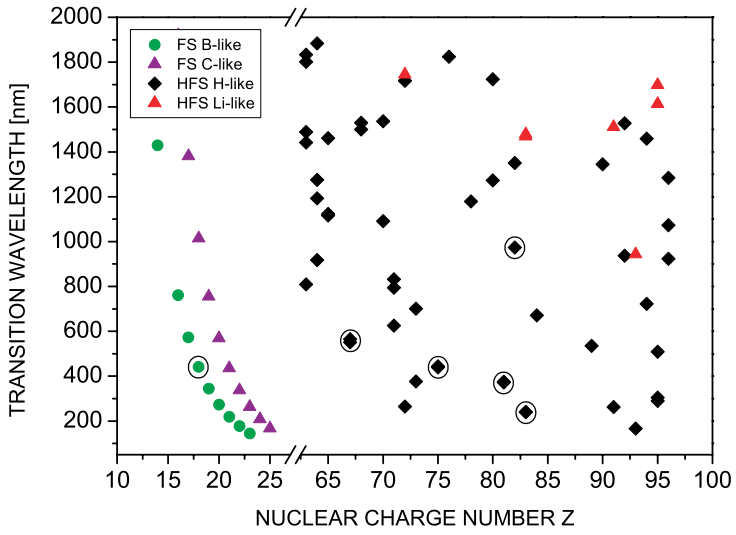

Figure 1. Estimated wavelengths of FS and HFS transitions in highly charged ions as a function of the nuclear charge number Z. With the encircled ions, successful measurements have been performed. For details see text.

greater than a year). The wavelengths have been calculated according to Beier [25] and are good within a few percent. Laser spectroscopy measurements have been performed for the encircled ions, i.e. the ground-state (1s) HFS in hydrogen-like ions has previously been measured in $^{165}Ho^{66+}$ [30], $^{185,187}Re^{74+}$ [31], $^{203,205}Tl^{80+}$ [32], $^{207}Pb^{81+}$ [33, 34] and $^{209}Bi^{82+}$ [34, 35]. Ground-state (2s) HFS measurements in lithium-like bismuth $^{209}Bi^{80+}$ have been performed [36, 37], but the results were inconclusive. FS measurements have been performed in medium–heavy highly charged ions, see for example [29] and references therein. However, the relative precision of these measurements is limited to about 10^{-4} due to the high particle velocities and poor signal-to-noise ratio of the optical fluorescence detection.

A measurement scheme has been outlined which will allow optical fluorescence measurements with a cloud of well-localized particles in a Penning trap nearly at rest [38]. This scheme reduces the Doppler width and shift to a level of $\Delta\lambda_{OPT}/\lambda_{OPT} = 10^{-7}$ of the measured transition, which is three orders of magnitude better than in any previous experiment. This scheme is applicable to a variety of ions depending on the availability of excitation lasers and particularly optical detection devices for the required wavelengths.

The concept presented here allows FS and HFS measurements with accuracies exceeding 10^{-10}. Since only a single particle is involved, also rare isotopes and ions which are not readily produced at high rates can be investigated. Single-particle confinement avoids ion–ion interaction and allows for extended measurement times thus increasing the possible accuracy. Furthermore, the method is advantageous especially in transition wavelength regions where suitable detectors are unavailable or involve tremendous experimental effort, which is true mainly in the infrared region.

3. Ion oscillation frequencies and their energy dependence

In a Penning trap, charged particles are confined by a superposition of a homogeneous magnetic field with an electrostatic potential. For detailed discussions of trapping techniques, trap designs

and particle motions, see e.g. [16], [39]–[41]. In the following, we discuss the trapping of a single ion in a cylindrical Penning trap as described in detail in [41]. Such a trap has cylindrical symmetry along the field lines (z-axis) of the homogeneous magnetic field which radially confines the ion. Axially, the ion is confined by a constant positive voltage V_0 applied between the central ring electrode and the endcap electrodes. Additionally, compensation electrodes are placed on either side of the ring between the ring and the endcaps. A voltage V_C is applied to these electrodes to create a harmonic potential around the trap centre. In such a configuration, an ion performs three independent motions with well-defined frequencies ω_z ('axial frequency'), ω_+ ('modified cyclotron frequency') and ω_- ('magnetron frequency'). The axial frequency ω_z is given by

$$\omega_z^2 = \frac{q V_0 C_2}{m z_0^2}, \tag{1}$$

where q is the particle charge, V_0 is the trapping voltage, m is the particle mass and z_0 is the endcap distance (C_2 will be explained below). For the motion in the radial plane, the modified cyclotron frequency is given by

$$\omega_+ = \frac{\omega_c}{2} + \left(\frac{\omega_c^2}{4} - \frac{\omega_z^2}{2}\right)^{1/2}, \tag{2}$$

where ω_c is the free cyclotron frequency given by

$$\omega_c = \frac{q B_0}{m} \tag{3}$$

and B_0 is the field strength of the homogeneous magnetic field used for trapping. The magnetron frequency is not of interest for the present discussion. There is negligible energy transfer between the characteristic motions such that their amplitudes are independent and different temperatures can be assigned to the different motions of a single particle [42]. In the absence of imperfections, the motions are harmonic and thus the trapping frequencies are independent of the corresponding motional energies. Usually, the experimental parameters are chosen with great care such that this is the case. However, here we are interested in a special combination of energy dependences that are produced by intentionally introduced additional field components.

Let us first assume the presence of a magnetic inhomogeneity of the kind $\vec{B} = B_2\left((z^2 - r^2)/2\hat{e}_z - z\vec{r}\right)$ with $B_2 > 0$ superimposed on the magnetic trapping field B_0. $\hat{e}_z$ is the unit vector along the z-axis (trap axis) and $\vec{r}$ is the radial coordinate such that the inhomogeneity has radial symmetry around the trap centre. This configuration is called a 'magnetic bottle' and is discussed in detail for example in [19]. The presence of $B_2 \neq 0$ results in a dependence of the trapping frequencies on the motional energies, i.e. the frequencies shift with the energy (amplitude) of the motion. The relative shifts $\Delta\omega_z/\omega_z$ and $\Delta\omega_+/\omega_+$ of the trapping frequencies ω_+ (modified cyclotron frequency) and ω_z (axial frequency) due to corresponding finite motional energies E_+ and E_z are given by

$$\begin{pmatrix} \Delta\omega_+/\omega_+ \\ \Delta\omega_z/\omega_z \end{pmatrix} = \frac{1}{m\omega_z^2}\frac{B_2}{B_0}\begin{pmatrix} -(\omega_z/\omega_+)^2 & 1 \\ 1 & 0 \end{pmatrix}\begin{pmatrix} E_+ \\ E_z \end{pmatrix}. \tag{4}$$

This means that both frequencies depend linearly on both energies except for the axial frequency which does not depend on the axial energy (the corresponding matrix element is zero). We will make use of this later.

Now we consider an anharmonicity of the electrostatic potential which near the trap centre can be described by the expansion [41]

$$V = \frac{1}{2} V_0 \sum_{k=0}^{\infty} C_k \left(\frac{r}{d}\right)^k P_k(\cos\theta), \tag{5}$$

where the $P_k(\cos\theta)$ are Legendre polynomials and $d^2 = (z_0^2 + \rho_0^2/2)/2$ is a characteristic trap dimension [41] determined by the endcap distance z_0 and the inner trap radius ρ_0. For the present discussion, it is sufficient to include the dimensionless expansion coefficient C_2 and to account for electric imperfections characterized by C_4, since higher-order imperfections are negligible. The coefficients can be written as [41]

$$C_2 = C_2^{(0)} + D_2 \frac{V_C}{V_0}, \tag{6}$$

$$C_4 = C_4^{(0)} + D_4 \frac{V_C}{V_0}, \tag{7}$$

where V_C is the voltage applied to the correction electrodes of the trap and V_0 is the ring voltage defining the trap depth. Electric imperfections due to $C_4 \neq 0$ lead to relative shifts $\Delta\omega_z/\omega_z$ and $\Delta\omega_+/\omega_+$ of the trapping frequencies ω_+ and ω_z due to corresponding finite motional energies E_+ and E_z:

$$\begin{pmatrix} \Delta\omega_+/\omega_+ \\ \Delta\omega_z/\omega_z \end{pmatrix} = \frac{6C_4}{qV_0} \begin{pmatrix} \frac{1}{4}(\omega_z/\omega_+)^4 & -\frac{1}{2}(\omega_z/\omega_+)^2 \\ -\frac{1}{2}(\omega_z/\omega_+)^2 & \frac{1}{4} \end{pmatrix} \begin{pmatrix} E_+ \\ E_z \end{pmatrix}. \tag{8}$$

For typical trap parameters (as e.g. given in [41]) the relation $\omega_z \ll \omega_+ \approx \omega_c$ holds. When using this and the relations given in equations (1) and (3), the absolute shift of the modified cyclotron frequency can be written as

$$\Delta\omega_+(E_z) = \left(\frac{z_0^2}{mV_0}\frac{1}{C_2}B_2 - \frac{3}{qB_0 z_0^2}C_2C_4\right) E_z, \tag{9}$$

$$\Delta\omega_+(E_+) = \left(-\frac{1}{qB_0^2}B_2 + \frac{3}{2}\frac{mV_0}{q^2 z_0^4 B_0^3}C_2^2C_4\right) E_+, \tag{10}$$

where the first term describes the magnetic shift and the second term the electric shift, respectively. Similarly, for the axial frequency we find

$$\Delta\omega_z(E_z) = \left(0B_2 + \frac{3}{2}\frac{1}{(qV_0m)^{1/2}z_0}C_2^{1/2}C_4\right) E_z, \tag{11}$$

$$\Delta\omega_z(E_+) = \left(\frac{z_0}{(mqV_0C_2)^{1/2}B_0}B_2 - \frac{3V_0^{1/2}m^{1/2}}{q^{3/2}z_0^3B_0^2}C_2^{3/2}C_4\right) E_+. \tag{12}$$

For the envisaged measurement the optimum trapping parameters are such that the dependence of ω_+ on E_z is strong while the dependence of ω_z on E_z is zero. According to equations (9) and (11), this is achieved by maximizing B_2, minimizing V_0 and tuning C_4 to be zero by appropriate choice of the voltage ratio V_C/V_0 [41]. A magnetic field inhomogeneity B_2 is readily produced by a ferromagnetic cylindrical ring electrode. For trap geometries like the hybrid design in [43], $B_2 \approx 400\,\mathrm{mT\,mm^{-2}}$ have been achieved.

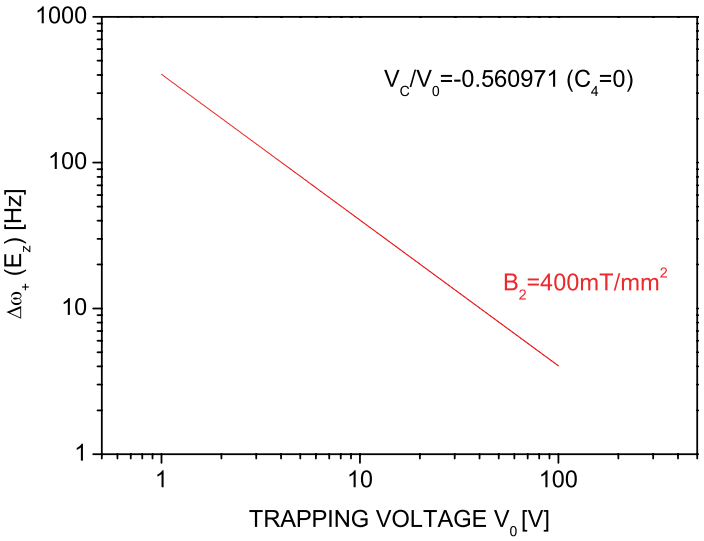

Figure 2. Expected shift of the modified cyclotron frequency ω_+ of a stored ion in a Penning trap due to a magnetic field inhomogeneity characterized by B_2 as a function of the trapping voltage V_0.

Let us now assume the cooling of a single trapped ion from an energy corresponding to 4 K (initial ion energy upon resistive cooling) to an energy corresponding to, say, 400 μK, which is a conservative estimate of a laser cooling limit for the given situation. The corresponding shift in ω_+ according to equation (9) can for shallow trap potentials amount to a few hundreds of Hz, as shown in figure 2. For potentials of order 100 V the shift is still close to 10 Hz. For $B_0 = 1$ T the modified cyclotron frequency ω_+ is of order MHz such that the relative shift is of order 10^{-6}. Shifts of this magnitude can easily be detected by a Fourier analysis of the ion signal picked up with an electronic resonance circuit tuned to the ion's oscillation frequency [19]. Much smaller relative shifts down to a few 10^{-10} can still be detected by a phase-sensitive detection scheme as described in [20]. Within this scheme, frequencies are distinguished by a corresponding phase difference. Since the frequencies are not measured, the scheme is not subjected to the Fourier limit and thus allows one to resolve sub-Hz frequency shifts on the sub-second time scale.

4. Laser cooling

Laser cooling of single trapped ions has previously been demonstrated successfully, see e.g. [17, 18] and references therein. In those measurements, a single ion has been laser cooled even to the quantum-mechanical ground state of the ion motion in the trap. Usually, strong transitions are used for efficient (fast) laser cooling. Here, magnetic dipole (M1) transitions with Γ of the order of kHz or below will be used. The transition rate (linewidth) for a magnetic dipole (M1) transition from the excited to the lower state is given by [44]

$$\Gamma = \frac{4\alpha\omega^3\hbar^2 I\,(2\kappa+1)^2}{27 m_e^2 c^4\,(2I+1)}, \tag{13}$$

where α is the FS constant, I is the nuclear spin and $\kappa = \sqrt{1-Z^2\alpha^2}$. For $^{209}Bi^{82+}$ this rate is $\Gamma \approx 2500\,s^{-1}$, for ions such as $^{207}Pb^{81+}$ or $^{209}Bi^{80+}$ it is lower.

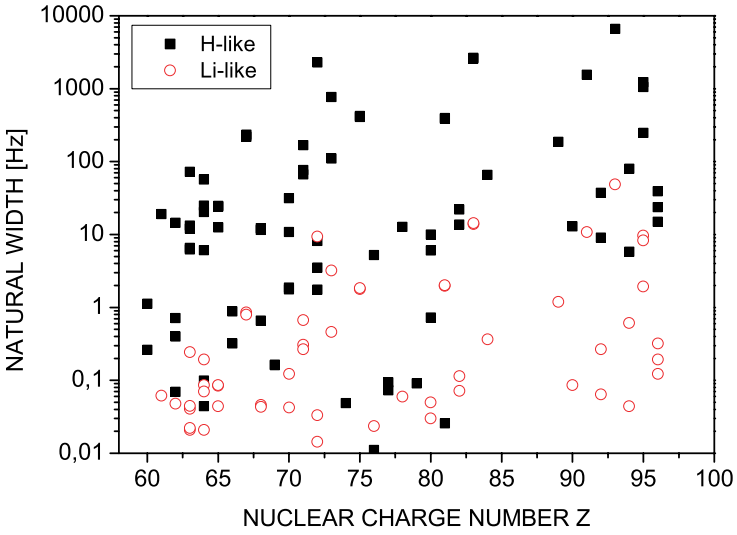

Figure 3. Natural linewidth Γ of the HFS ground-state transition of all H-like and Li-like isotopes which are stable or have nuclear half-lives of more than one year.

Figure 3 shows the natural linewidth Γ of the HFS ground-state transition of all H-like and Li-like isotopes with nuclear half-lives of more than one year. The ions with highest optical transition rates Γ are $^{233}Pa^{90+}$ (7480 s^{-1}), $^{212}Fr^{86+}$ (6890 s^{-1}), $^{237}Np^{92+}$ (6600 s^{-1}), $^{231}Pa^{85+}$ (3750 s^{-1}), $^{196}Au^{78+}$ (3550 s^{-1}) and all odd isotopes of bismuth $^{odd}Bi^{82+}$ (2500–3700 s^{-1}).

Laser cooling of the axial motion of a single ion in a Penning trap is achieved by a red-detuned narrow-band laser directed along the trap axis. The laser frequency ω_L is chosen to match a lower sideband of the optical transition at ω_{OPT}. Motional sidebands appear since the axial frequency of the ion is much higher than the transition rate ($\omega_z \gg \Gamma$). This situation is called 'fast particle limit', since the ion motion is fast compared to the timescale of the decay. The ion oscillates many times during the decay process and thus sidebands appear around ω_{OPT} ('carrier frequency') at integer multiples of the axial frequency ω_z. Narrow-band laser irradiation at the frequency of a sideband below the transition cools the particle motion, while irradiation at a sideband frequency above heats it. A detailed account of this is found in [16, 39].

In principle, sidebands appear at all integer multiples of ω_z, however, the number of sidebands with sufficient strength depends on the temperature of the axial motion and is limited. The distribution of relative strengths S_n is given by [16]

$$S_n = \left| J_n\left(\frac{a_z}{\lambda_{OPT}}\right)\right|^2, \tag{14}$$

where the J_n are Bessel functions and a_z is the energy- (temperature-) dependent amplitude of the axial motion given by

$$a_z = \left(\frac{2z_0^2}{qV_0C_2}E_z\right)^{1/2}. \tag{15}$$

The corresponding sideband spectrum can be calculated by [16]

$$I(\omega) = \sum_{n=-\infty}^{n=+\infty} |J_n(\eta)|^2 \frac{(\Gamma/2)^2}{(\Gamma/2)^2 + [\omega_{OPT} - (\omega + n\omega_z)]^2}, \tag{16}$$

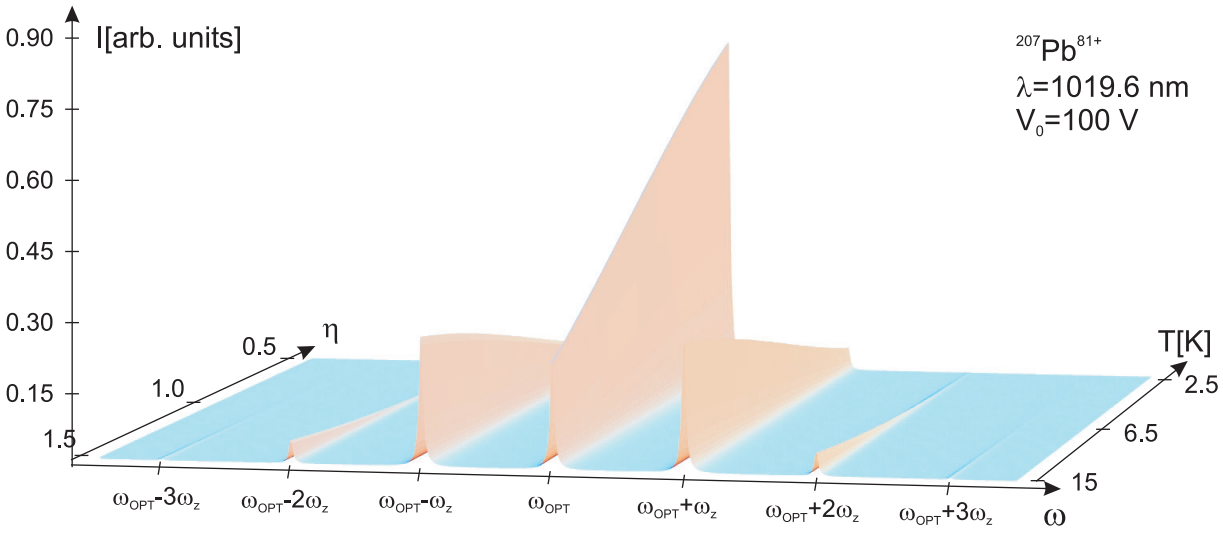

Figure 4. Sideband spectrum calculated according to equation (16) for a single $^{207}Pb^{81+}$ ion in a trap with $2z_0 = 5$ mm, $V_0 = 100$ V and $C_2 = 0.85$ as a function of the Lamb–Dicke parameter $\eta = a_z/\lambda_{OPT}$ and the axial ion temperature T, respectively.

where n is the line order ($n = 0$ is the carrier at $\omega = \omega_{OPT}$). The value of a_z for a trap with $2z_0 = 5$ mm, $V_0 = 100$ V, $C_2 = 0.85$ and an ion with $q = 80e$ is 395 nm $\times\sqrt{T[K]}$. For the ions in the present study, especially for transitions in the infrared domain, this means that at $T = 4$ K one is already in or very close to the so-called 'Lamb–Dicke regime', where the motional amplitude of the ion is smaller than the wavelength of the laser light ($a_z < \lambda_{OPT}$). In this situation, the only sidebands with relevant strengths are the ones of first or second order around the carrier, all higher-order ones fall to zero very rapidly [16]. Figure 4 shows the calculated sideband spectrum according to equation (16) for a single $^{207}Pb^{81+}$ ion in a trap with the above parameters as a function of the Lamb–Dicke parameter $\eta = a_z/\lambda_{OPT}$ and the axial ion temperature, respectively. As can be seen, even for ion temperatures above 4 K one is in the Lamb–Dicke regime and only first-order sidebands are of relevant strength.

The timescale of laser cooling can be estimated from simple reasoning: when the cooling laser is tuned to the nth sideband at $\omega_L = \omega_{OPT} - n\omega_z$, the average motional energy taken away from the ion by each fluorescence photon is $n\hbar\omega_z$. The photon scatter rate k can be estimated by $k \approx \Gamma S_n/2$. Thus, the time necessary to remove the motional energy E_z from the ion is roughly given by

$$t_{cool} \approx \frac{2E_z}{n\hbar\omega_z\Gamma S_n}. \tag{17}$$

This number is typically of the order of a few hundreds of seconds for the present cases. Since laser cooling requires a closed two-level system, an experiment on a single ion may require initial preparation of a suited sublevel by optical pumping. The prepared substrate has long radiative lifetimes (of the order of years when the M1 microwave transition to a lower Zeeman substate is considered). Thus, once prepared, the system will stay in the desired state even when the following cooling and measurement times are long. Since the closed two-level system consists of Zeeman substates of the hyperfine levels, it is necessary to determine the desired

hyperfine splitting from the measured, Zeeman-shifted, transition. This is straight-forward using the value of the magnetic field strength B_0 as determined from the measured cyclotron frequency and the corresponding Zeeman shift following from theory.

5. Measurement principle

5.1. Resistive cooling

A single ion is trapped and both the axial and modified cyclotron motion are resistively cooled to an energy corresponding to the surrounding heat bath temperature of 4 K. Resistive cooling takes place with a time constant of [16]

$$\tau_z = \frac{4(z_0\sqrt{m})^3}{L\,Q\sqrt{q^5 V_0}} \tag{18}$$

for the axial motion, and

$$\tau_{\mathrm{r}} = \frac{d^2 B_0 C}{q\,Q} \tag{19}$$

for the radial motion, where L is the inductance, C is the capacitance and Q is the quality factor of the tuned circuit used for cooling. Typical axial cooling times are of the order of 100 ms, radial cooling times are of the order of seconds for the present parameters. The spectral widths of the detection signals upon resonant pick-up and Fourier transformation are given by the corresponding cooling time constants [45]. Since presently the axial and radial cooling time constants are comparable and sufficiently small, it is possible to employ the same frequency measurement technique [19, 45] for both motions. The main feature of such a measurement is that it is not necessary to artificially excite the ion motion to produce a detectable signal. The result of a single measurement is a frequency spectrum with a single peak at the radial frequency of the ion depending on the axial ion energy and with a peak height proportional to the ion's radial energy [19].

The resonant circuits used for resistive cooling and signal pick-up can be switched (e.g. using Q-switches) such that their resonance frequency either matches the ion's oscillation frequency or is far detuned and does not interact with the ion. The circuits can be used for a very precise measurement of the motional frequencies (on the sub-Hz level), particularly of the axial frequency that represents the sideband separation. After resistive cooling of the ion to 4 K, the axial circuit is detuned while the cyclotron frequency ω_+ is continuously observed. As previously discussed, ω_+ depends significantly on the axial energy E_z while the axial frequency and thus the sideband spacing does not depend on E_z.

5.2. Cooling laser scan

Laser light is irradiated axially and the frequency region around the desired transition is scanned. The bandwidth of the laser must be smaller than the sideband separation, i.e. smaller than ω_z. If the laser frequency is in resonance with a lower sideband, the ion is laser cooled and the observed ω_+ shifts. If the laser frequency is in resonance with an upper sideband, the ion is heated resulting in a shift of ω_+ in the opposite direction. Since within the Lamb–Dicke regime only one or two sidebands on either side of the carrier are of relevant (and predictable) strength [16], it is possible to unanimously identify the first sideband on either side of the

carrier by the sign and relative rate of the observed frequency shift. The electronically measured axial frequency (i.e. the sideband spacing) can then be used to precisely determine the desired atomic transition frequency. The frequency uncertainty due to the electronic measurement of the sideband spacing is below 1 Hz and thus irrelevant compared with the optical widths. Note that while ω_+ depends on E_z, the energies (and thus amplitudes) of the axial and radial motions are independent and therefore the amplitude of the detection signal at ω_+ is not changed while the axial motion is cooled by the laser.

For the proposed scheme it is not necessary to perform laser cooling to the quantum mechanical ground state. Assuming a relative frequency shift $\Delta\omega_+/\omega_+$ of the order of 10^{-6} for cooling between 4 K and, say, 400 μK (see section 3) and given a detection sensitivity in $\Delta\omega_+/\omega_+$ of some 10^{-10}, already cooling by a few tens of mK is sufficient for a visible effect. Thus, it is not necessary to perform laser cooling for the time t_{cool} of several hundreds of seconds as given by equation (17), but a time of few tens of seconds is expected to be sufficient. In previous measurements using a non-optimized implementation of the phase-sensitive frequency distinction, it was possible to resolve a relative shift of 10^{-7} in a time of 0.8 s [20]. An optimized implementation is estimated to be better by about two orders of magnitude, resulting in a single scan measurement time of several seconds necessary to reach a sensitivity of 10^{-10}. This time is comparable to the single-scan measurement time expected in trap-assisted spectroscopy by detection of fluorescence photons, as e.g. described in [38].

5.3. Obtainable precision and systematic effects

Since the radial frequency ω_+ has a dependence on the radial energy E_+ as given by equation (9), it is in principle subjected to fluctuations on the scale below 1 meV due to the Boltzmann-distribution of energies at the ambient temperature of 4 K. The ion is coupled to the heat bath of the tuned circuit and fluctuations of the ion energy within the Boltzmann-distribution due to the coupling occur on the cooling time scale τ as given by equation (19). In practice, it is therefore favourable to employ a highly dissipative tuned circuit for the initial cooling of the radial motion (i.e. one with small τ), while a poorly dissipative (inductively coupled) circuit is used for the actual frequency measurement. Thus, thermal frequency fluctuations of ω_+ occur on long time scales and do not obstruct the visibility of radial frequency changes due to the effect of axial laser cooling. Note that the axial frequency is not affected by this since it is decoupled from circuits after initial resistive cooling.

Typical fluctuations of the trapping voltage V_0 on the 10^{-6}-level and typical fluctuations of the magnetic field strength B_0 on the 10^{-9}-level lead to a sub-Hz effect on the axial and on the observed radial frequency ω_+. Thus, the relative fluctuations of ω_+ are of the same order as the maximum sensitivity of the frequency shift measurement and do not limit it further. With this, laser cooling times on the scale of seconds are expected to be sufficient for a detection of the cooling effect. The sub-Hz fluctuation and measurement uncertainty of the axial frequency ω_z changes the position of the sidebands of ω_{OPT} by that amount, but this effect is relevant only on the 10^{-15} level of accuracy. The same is true for the effect of the fluctuating field B_0 on the Zeeman levels. Most relevant for the overall accuracy of the determination of ω_{OPT} are the width and stability of the scanning (cooling) laser and the accuracy to which the Zeeman shift can be accounted for. Assuming laser stabilities and bandwidths significantly below 1 MHz, the relative precision in ω_{OPT} is better than 10^{-10}. Such a sensitivity allows even to 'weigh' optical excitations [46] in light ions due to the energy–mass relation $E = mc^2$: from equation (9) it

follows that $\Delta\omega_+/\omega_+ \propto E/m$ such that an optical excitation by a few eV translates into a mass shift and thus into a detectable relative frequency shift of order 10^{-10} for ions lighter than a few tens of GeV c^{-2}, i.e. lighter than a few tens of atomic mass units. This is especially applicable to metastable states or to continuously driven optical transitions in ions.

A possible source of systematic errors in the determination of the transition wavelength could be the measurement of the cooling laser frequency itself. However, already with commercial wavemeters, absolute accuracies of MHz are possible. With the use of a commercial frequency comb it is possible to even perform an absolute measurement of optical frequencies with a relative uncertainty of 10^{-12} or better. A different source of systematic uncertainties is the calculated Zeeman shift used to determine the carrier frequency (i.e. transition frequency) from the measured sideband frequency. Currently, the Zeeman shift can be determined with relative precisions on the 10^{-7} scale, typically leading to uncertainities of the Zeeman-shifted levels of the order of some kHz, which therefore are also not relevant above the 10^{-10} level of accuracy.

We believe it is also worth noting that the experimental setup necessary for the presented measurement concept is nearly identical to the one used for precision measurements of electronic magnetic moments [6, 7], with the only exception that the axial cooling laser replaces the microwave radiation used in those experiments. At the same time, all single technical implementations and techniques such as trapping of single ions, resistive and laser cooling of confined single ions, resonant pickup of single-ion oscillation signals and the phase-sensitive detection of small frequency differences are well established and have been proven to work.

6. Conclusion

We have presented a concept for laser spectroscopy on a single ion by a radiofrequency measurement of the ion oscillation in a Penning trap. The present method allows a kind of 'blind spectroscopy', in the sense that detection of fluorescence photons is replaced by measuring the effect of laser cooling on the ion oscillation. We have discussed an application to the precision spectroscopy of forbidden transitions in highly charged ions, allowing stringent tests of bound-state QED calculations including nuclear recoil effects. The method is advantageous since only a single particle is involved, thus allowing investigations on ions which are not readily produced at high rates. Furthermore, measurements can be performed also in transition wavelength regions where detectors suitable for trap-assisted spectroscopy are unavailable, e.g. in the infrared. The corresponding candidate ions can be seen in figure 1. Finally, the accuracy obtainable in a single-ion approach of better than 10^{-10} by far exceeds that of any other experimental concept.

Acknowledgments

We are grateful for inspiring discussions with R Thompson (Imperial College London), W Nörtershäuser (GSI) and D L Moskovkin (St Petersburg).

References

[1] Demtröder W 1996 *Laser Spectroscopy* (Berlin: Springer)
[2] Dehmelt H G 1988 *Z. Phys.* D **10** 127
[3] Odom B, Hanneke D, D'Urso B and Gabrielse G 2006 *Phys. Rev. Lett.* **97** 030801
[4] Gabrielse G *et al* 2006 *Phys. Rev. Lett.* **97** 030802

[5] Gabrielse G *et al* 2007 *Phys. Rev. Lett.* **99** 039902
[6] Häffner H *et al* 2000 *Phys. Rev. Lett.* **85** 5308
[7] Verdú J *et al* 2004 *Phys. Rev. Lett.* **92** 093002
[8] Oskay W H *et al* 2006 *Phys. Rev. Lett.* **97** 020801
[9] Nagourney W, Sandberg J and Dehmelt H 1986 *Phys. Rev. Lett.* **56** 2797
[10] Neuhauser W, Hohenstatt M, Toschek P E and Dehmelt H 1980 *Phys. Rev.* A **22** 1137
[11] Oskay W H *et al* 2006 *Phys. Rev. Lett.* **97** 020801
[12] Schneider T, Peik E and Tamm C 2005 *Phys. Rev. Lett.* **94** 230801
[13] Gill P *et al* 2004 *Phys. Scr.* **T112** 63
[14] Young B C *et al* 1999 *Phys. Rev. Lett.* **82** 3799
[15] Webster S A, Oxborrow M and Gill P 2004 *Opt. Lett.* **29** 1497–1499
[16] Major F G, Gheorghe V N and Werth G 2004 *Charged Particle Traps* (Berlin: Springer)
[17] Diedrich F *et al* 1989 *Phys. Rev. Lett.* **62** 403
[18] Bergquist J C *et al* 1987 *Phys. Rev.* A **36** 428
[19] Häffner H *et al* 2003 *Eur. Phys. J.* D **22** 163
[20] Stahl S *et al* 2005 *J. Phys. B: At. Mol. Opt. Phys.* **38** 297
[21] Shabaev V M 1994 *J. Phys. B: At. Mol. Opt. Phys.* **27** 5825
[22] Shabaev V M, Shabaeva M B and Tupitsyn I I 1995 *Phys. Rev.* A **52** 3686
[23] Shabaev V M *et al* 1997 *Phys. Rev.* A **56** 252
[24] Sunnergren P *et al* 1998 *Phys. Rev.* A **58** 1055
[25] Beier T 2000 *Phys. Rep.* **339** 79
[26] Shabaev V M *et al* 2000 *Hyperfine Interact.* **27** 279
[27] Sapirstein J and Cheng K T 2001 *Phys. Rev.* A **63** 032506
[28] Shabaev V M *et al* 2001 *Phys. Rev. Lett.* **86** 3959
[29] Draganic I *et al* 2003 *Phys. Rev. Lett.* **91** 183001
[30] Crespo López-Urrutia J R *et al* 1996 *Phys. Rev. Lett.* **77** 826
[31] Crespo López-Urrutia J R *et al* 1998 *Phys. Rev.* A **57** 879
[32] Beiersdorfer P *et al* 2001 *Phys. Rev.* A **64** 032506
[33] Seelig P *et al* 1998 *Phys. Rev. Lett.* **81** 4824
[34] Borneis S *et al* 2000 *Hyperfine Interact.* **127** 305
[35] Klaft I *et al* 1994 *Phys. Rev. Lett.* **73** 2425
[36] Beiersdorfer P *et al* 1998 *Phys. Rev. Lett.* **80** 3022
[37] Beiersdorfer P *et al* 2007 private communication
[38] Vogel M, Winters D F A, Segal D and Thompson R C 2005 *Rev. Sci. Instrum.* **76** 103102
[39] Ghosh P K 1995 *Ion Traps (International Series of Monographs in Physics)* (Oxford: Oxford University Press)
[40] Brown L S and Gabrielse G 1986 *Rev. Mod. Phys.* **58** 233
[41] Gabrielse G, Haarsma L and Rolston S L 1989 *Int. J. Mass Spectrom. Ion Process.* **88** 319
[42] Djekic S *et al* 2004 *Eur. Phys. J.* D **31** 451
[43] Verdu J *et al* 2005 *AIP Conf. Proc.* **796** 260
[44] Schneider S M, Greiner W and Soff G 1994 *Z. Phys.* D **31** 143
[45] Wineland D J *et al* 1975 *J. Appl. Phys.* **46** 919
[46] DiFilippo F, Natarajan V, Boyce K R and Pritchard D E 1999 *Phys. Rev. Lett.* **73** 1481